Brønsted acidity of amorphous silica–aluminas studied by ^{1}H NMR

Lara Heeribout, Robert Vincent, Patrice Batamack, Claudine Dorémieux-Morin and Jacques Fraissard *

Laboratoire de Chimie des Surfaces, UPES-A 7069, Université Pierre et Marie Curie, Case 196, 4 place Jussieu, 75252 Paris Cédex 05, France
E-mail: jfr@ccr.jussieu.fr

Received 23 April 1997; accepted 6 May 1998

^{1}H broad-line (4 K) and MAS (room temperature) NMR have been used to study the acid strength of two amorphous silica–aluminas interacting or not with adsorbed water. The study is more difficult than for zeolites, because the acidic SiO(H)Al bridges are reversibly destroyed by dehydration. However, an acidity coefficient value (H_3O^+ concentration per Brønsted acid site when one water molecule interacts with each Brønsted site) of $0.34 \pm 10\%$ has been determined. This value is equal to that obtained for H-faujasite and H-mordenite samples with Si/Al ratios high enough for maximum acid strength.

Keywords: silica–alumina, Brønsted acidity of solids, ^{1}H broad-line NMR, ^{1}H MAS NMR, acidity coefficient

1. Introduction

Because of their acidic properties, amorphous silica–aluminas (denoted ASA) have long been appreciated as catalysts in cracking processes. For many of their uses, they have been replaced by zeolites which have better thermal stability and whose structure is better defined [1,2]. Nevertheless, the interest in ASA remains because of their presence in industrial catalysts, for example, as binders, as supports for other catalysts with low specific surface area and as amorphous phases inside zeolites due to steaming of these zeolites.

Without going over the rich chemical literature on ASA, we wish to focus on their study by multinuclear solid-state NMR [3–5]. Eckert [4] has summarized the following practical knowledge: "solid-state NMR studies of silica–aluminas have addressed the structural origins of their activity and have served to characterize the surface acidities".

Many results have been obtained by ^{1}H MAS NMR. Hunger et al. [6,7] related the results of a ^{1}H MAS NMR study of partially dehydrated home-prepared ASAs to their catalytic activity expressed by the rate of cumene cracking. They noted two lines in the spectrum, at about 2 and 7 ppm. The 2 ppm line was attributed to non-acidic SiOH groups and the 7 ppm one to acidic H atoms. Much literature has more recently been devoted to the attribution of signals between 6 and 7 ppm in the spectra of silica, silica–aluminas and zeolites. This position may correspond to H atoms of silanols or bridging acidic sites in strong electrostatic interaction with framework O atoms [8–10]. We will not go into these results in detail, because we have not observed such signals in this study.

A broad signal has been reported at about 3 ppm, attributed to AlOH groups [5,11], in the ^{1}H MAS spectra of dehydrated, but not dehydroxylated, silica–aluminas. These AlOH groups give bridging acidic sites SiO(H)Al groups (denoted bas) in the presence of molecular water. It is likely that these bas groups, stabilized by hydration, are reversibly destroyed by low-temperature evacuation [11] (figure 1).

The two ASAs described in this paper have been previously studied by high-resolution multinuclear NMR [5]. Both samples contain Al hexa- and tetra-coordinated to O atoms, as shown by ^{27}Al MAS NMR. The results from ^{29}Si MAS and CP-MAS NMR experiments show that both samples contain $\underline{\text{Si}}$ atoms of the type $(SiO)_2\underline{Si}(OH)_2$. Moreover, ^{1}H MAS NMR spectra of HS indicated the presence of microdomains with the faujasite structure.

We previously proposed a method for measuring the Brønsted acid strength of solids, based on the hydroxonium concentration per acid site when water interacts with these sites [12]. ^{1}H NMR, both magic angle spinning at room temperature and broad-line at 4 K with simulation of the spectra, were used. As already mentioned, MAS NMR can be used to determine the nature and concentrations of the different types of OH groups present in the samples without any adsorbed phase (these samples are said to be "anhydrous"). When water has been adsorbed and at temperatures where MAS can be performed, a fast H atom chemical exchange occurs between all the interacting oxyhydrogenated species, giving for them a single chemical shift value [13] which depends especially on inter-species hydrogen bonds. On the other hand, broad-line NMR at 4 K gives, by spectrum simulation, the concentrations of the oxyhydrogenated species. To summarize, the basic

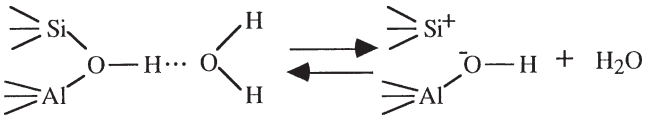

Figure 1. Scheme for the reversible destruction of ASA Brønsted acid site groups by vacuum low-temperature dehydration.

* To whom correspondence should be addressed.

physical effect is a dipolar magnetic interaction between any couple of two protons, proportional to r^{-3}, where r is the distance between the protons [14]. This effect allows us to characterize and quantify magnetic configurations of nearest protons the numbers and intra-pair H–H distances of which are typical of either water molecules, hydroxonium ions, hydrogen-bonded complexes ($H_2O\cdots HO$) or OH groups [12]. The hydroxonium ion concentration, when each bas interacts with one water molecule giving either H_3O^+ or $H_2O\cdots HO$, is denoted the "acidity coefficient", χ_a [12]. It must be noted that we previously used another definition of this coefficient, α_a [15,16], which was the ion concentration when one water molecule was adsorbed per bas. The values corresponding to the two definitions coincide in many cases.

Using both ^{1}H NMR techniques we wish to compare the acid strength of ASA with that of zeolites.

2. Experimental

The two samples studied were:

(i) HS, from Ketjen, with a "high silica" content (w/w Si/Al ratio 75/25); its specific surface area, which was previously 460 m^2/g [5], was found to be reduced to 345 m^2/g; its total "water equivalent" concentration per Al_2O_3 group (including OH groups, water and the species formed by their interaction) was also reduced in the same proportion, giving

$$5.1\ SiO_2,\quad 1.0\ Al_2O_3,\quad 1.5\ H_2O;$$

(ii) LS, from Rhône Poulenc, with a "low silica" content (w/w Si/Al ratio 25/75):

$$0.57\ SiO_2,\quad 1.0\ Al_2O_3,\quad 1.0\ H_2O,$$

with 310 m^2/g specific surface area, reduced by only 8% from [5].

Most of the experimental conditions are described extensively in the appendix. Only the main features are given here.

Samples are sealed in thin-glass tubes for the NMR experiments. Some of them were previously "shallow-bed" pretreated (10^{-2} Pa) at 623 K in order to make them "anhydrous", i.e., dehydrated, but still containing OH groups at their initial concentration. Water was "adsorbed" on anhydrous ASA as usual for zeolites [17]. Other samples were prepared by partial dehydration in vacuum with or without gentle heating. The remaining water in these samples, which can be extracted without OH group condensation, will also be denoted "adsorbed" water in the following. The samples were subsequently homogenized at 383 K for 15 h. Samples equilibrated in air were also studied. It will be shown below that the pretreatment conditions have no effect upon the results.

MAS spectra were recorded at 400 MHz with 3 kHz spinning rate; 100 free induction decays were accumulated with a delay between consecutive pulses of 20 s for "anhydrous" and 5 s for hydrated samples.

The conditions for broad-line NMR experiments and spectrum simulation are given again in the appendix. The spectra are half the derivative of the resonance absorption energy versus the main magnetic field.

3. Results

3.1. ^{27}Al MAS NMR on fully hydrated samples

The previous results [5] were obtained using a MAS spinning rate of 4 kHz at 104.2 MHz: spinning side-bands were located between the main signals. The experiments were therefore repeated, on fully hydrated samples, with a 15 kHz spinning rate at 130.3 MHz. The new results agree with the old ones. The spectrum of HS contains three signals, at 4.4, 28.0 and 58.5 ppm attributable, from the literature, to Al atoms hexa-, penta- [18] (or tetra- with low symmetry [19]) and tetra-coordinated to oxygen, denoted $Al_{(n)}$ with $n = 4$, 5 and 6, respectively. The relative concentrations of these Al are 65, 33 and 2, respectively. The spectrum of LS contains only two signals, that of $Al_{(4)}$, 27%, being at 71.3 ppm and the other being characteristic of $Al_{(6)}$.

3.2. ^{1}H NMR

3.2.1. ^{1}H MAS NMR at room temperature

As already described [5,11], the ^{1}H MAS spectra of the "anhydrous" samples contain only two signals. For HS (figure 2(A)) and LS (figure 3(A)), a strong signal at 1.7 ppm, less than 300 Hz wide, is characteristic of silanols. Another, located at about 2.8 ppm, much wider (1.4 kHz) and weak, appears as a shoulder on the silanol signal; it is attributable to AlOH groups. Spinning side-bands are smaller for the silanol contribution than for the AlOH groups, though these last side-bands can be difficult to see because of their large width. No bas were found though, in metastable hydrated samples, they have been proved to exist (not yet hydrated) [5,11] and insofar as they interact with water molecules, as described below.

With increasing "adsorbed" water concentration, the qualitative evolution of the spectrum appears as continuous and similar for HS (figure 2) and LS (figure 3). The spectra show the following features: at first, the only change from the spectrum of the "anhydrous" sample is a small increase in the 2.8 ppm signal shift and intensity (figures 2 and 3, (B) and (C)); then, the silanol signal being still the largest, the second signal moves to about 5 ppm, its intensity and width (to 4 kHz) increasing (figure 2 (C), (D) and figure 3(C)). This second signal is typical of H atoms exchanging between oxyhydrogenated species formed by interaction of the (here reformed) bridging acid sites and water [13]. Finally, this signal continues to increase in intensity, its chemical shift being unchanged and its width decreasing (figure 2(E) and figure 3 (D) and (E)).

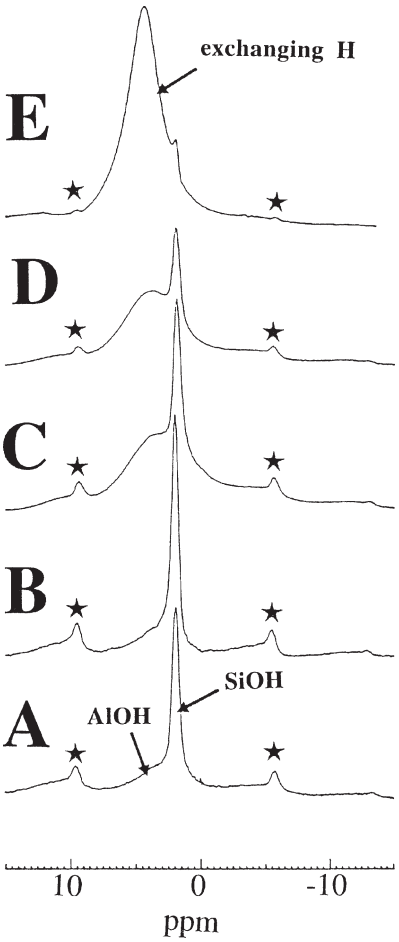

Figure 2. ^{1}H MAS NMR spectra of ASA HS. (A) "Anhydrous" sample; values of $H_{tot.}/Al_{(4+5)}$, whose meaning is given in the text, for the following samples: 0.54 (B); 2.48 (C); 2.77 (D); 4.3 (E). Asterisks denote spinning side-bands.

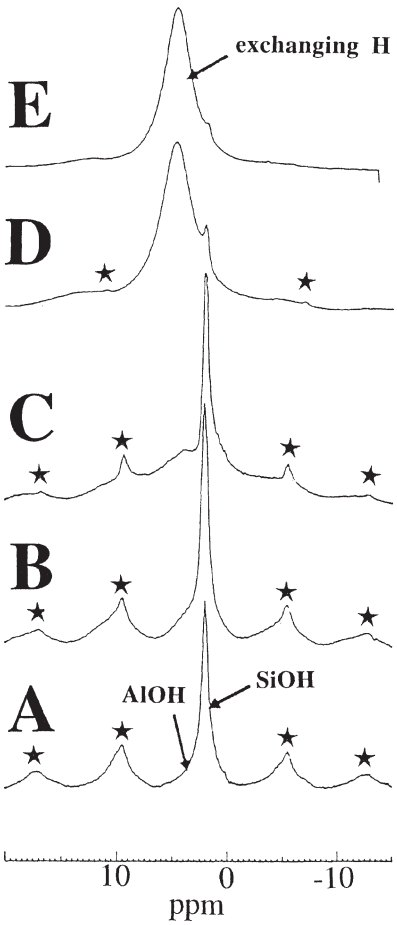

Figure 3. ^{1}H MAS NMR spectra of ASA LS. (A) "Anhydrous" sample; values of $H_{tot.}/Al_{(4)}$, whose meaning is given in the text, for the following samples: 0.48 (B); 0.92 (C); 3.04 (D); 3.70 (E). Asterisks denote spinning side-bands.

It must be mentioned that no signal corresponding to water adsorbed on Lewis acid sites of the type well characterized in zeolites [7,20] was observed.

3.2.2. ^{1}H broad-line NMR at 4 K

A qualitative description of the results is first proposed for the two samples on the basis of the ^{1}H broad-line NMR spectrum simulation. It will be followed by a discussion of the normalization of these results, from which the species concentrations can be determined.

The broad-line spectra of amorphous solids are poorly resolved compared to those of crystalline samples, in particular those of zeolites [12,13,15–17]. A striking result is that both ASA, either hydrated or not, contain paired OH groups with an intra-pair distance, r, of 210–230 ($\pm$10) pm (figures 4–9, tables 1 and 2).

The broad-line spectra of the "anhydrous" samples, HS (not shown) and LS (figure 4) show no contribution of molecular water. They were simulated using two contributions: a two-spin one, typical of the paired OH groups mentioned above, and either the derivative of a Gaussian function (for HS), or that of a Lorentzian (for LS).

For HS, the spectra of the two samples with the lowest H-"adsorbed" water concentrations (for example, figure 5) show the presence of hydrogen-bonded complexes, but not of hydroxonium ions (see the appendix for the determination of the nature of these species and the distance parameters in tables 1 and 2). However, the spectrum of HS equilibrated in air indicates that these ions and hydrogen-bonded complexes are present, this being noticed in two distinct simulations (figures 6 and 7). One of these simulations shows that there are water molecules not interacting with OH groups (figure 6), and the other no such water (figure 7). This is the first time that two different compositions of a sample appear as possible at this level of analysis, leading to an ambiguous situation. We will come back on this situation in section 4.

For LS in each of its two hydrated states (figures 8 and 9), the only possible model corresponds to the presence of all the species: H_3O^+, $H_2O\cdots HO$, H_2O and OH.

Our aim is to determine the "acidity coefficient", χ_a, which is equal to the hydroxonium ion concentration per bas, when one water molecule interacts with each bas. Therefore, we need to express the quantitative results per bas.

Table 1
Distance parameters (in pm) used for simulating ASA HS ^{1}H broad-line NMR experimental spectra.[a]

$H_{tot.}/Al_{(4+5)}$	H_3O^+			$(H_2O\cdots HO)$			H_2O		OH (Gaussian or	OH in pairs	
	r	r'	X	r	r'	X	r	X	Lorentzian)	r	X
4.30	153	164	200	160	233	237	165	205	G 290	210	280
4.30	156	167	200	161	233	237			G 300	228	245
2.77				161	233	237			L 0.75	210	280
2.48				161	233	257			L 0.75	210	279

[a] These spectra being not well resolved, the accuracy is less than for better defined samples; r, for water and hydroxonium ions, ± 3 pm; r, for OH groups, r' and X, ± 10 pm. For the Gaussian absorption, the distance, in pm (± 10), is the equivalent (in length) of the Gaussian coefficient in the magnetic field; for the Lorentzian, the parameter L is expressed in 10^{-4} T. The choice of the total H atom concentration (column 1) is explained in the text.

Table 2
Distance parameters (in pm) used for simulating ASA LS ^{1}H broad-line NMR spectra.[a]

$H_{tot.}/Al_{(4)}$	H_3O^+			$(H_2O\cdots HO)$			H_2O		OH (Gaussian)	OH in pairs	
	r	r'	X	r	r'	X	r	X		r	X
3.70	156	167	200	163	236	237	165	205	315	210	255
3.04	156	167	200	165	239	240	165	205	350	230	235

[a] The accuracy for each parameter is the same as in table 1. The choice of the total H atom concentration (column 1) is explained in the text.

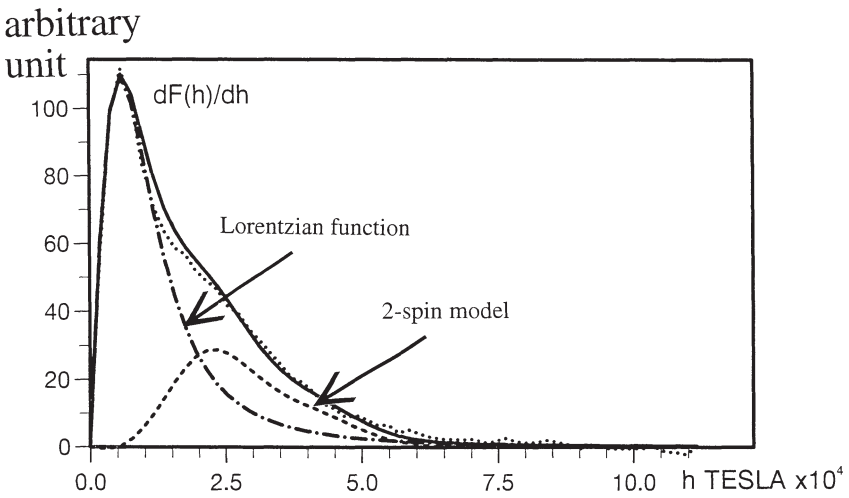

Figure 4. ^{1}H broad-line NMR spectra of "anhydrous" ASA LS: $(\cdots)$ experimental, (—) simulated, and partial contributions.

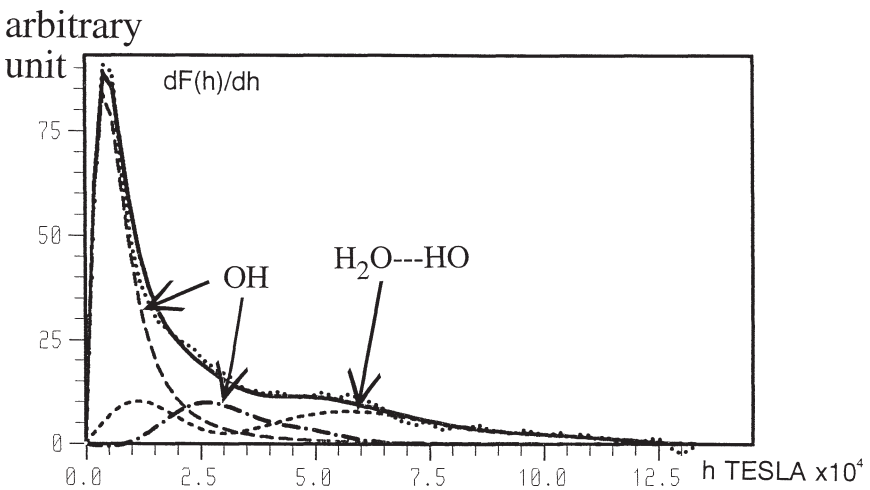

Figure 5. ^{1}H broad-line NMR spectra of ASA HS with $H_{tot.}/Al_{(4+5)} = 2.48$: $(\cdots)$ experimental, (—) simulated, and partial contributions.

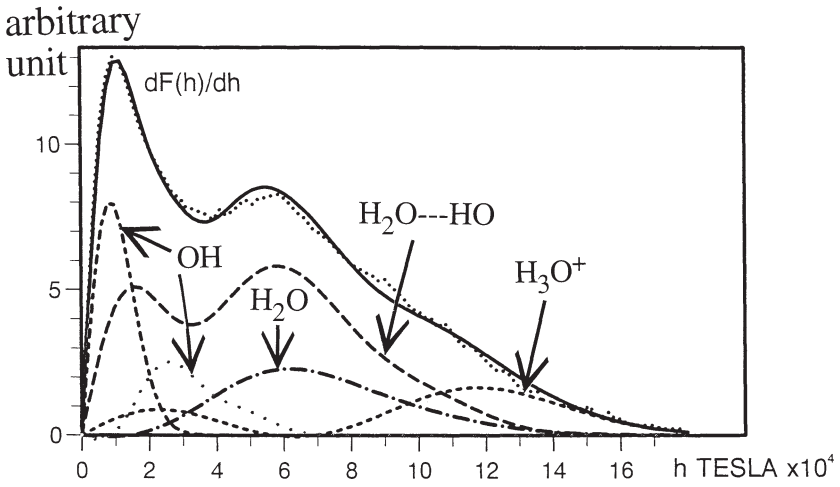

Figure 6. ^{1}H broad-line NMR spectra of ASA HS with $H_{tot.}/Al_{(4+5)} = 4.30$: (· · ·) experimental, (—) simulated *part of the water not interacting with OH groups*, and partial contributions.

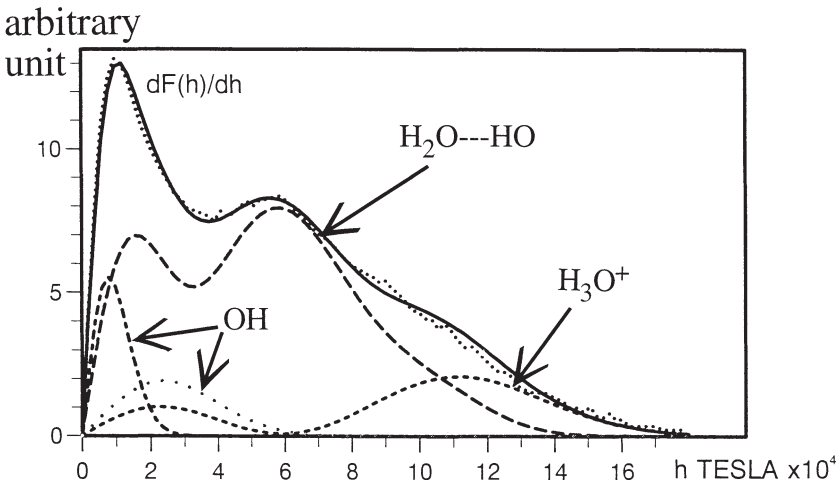

Figure 7. ^{1}H broad-line NMR spectrum of ASA HS with $H_{tot.}/Al_{(4+5)} = 4.30$: (· · ·) experimental, (—) simulated assuming *no water not interacting with OH groups*, and partial contributions.

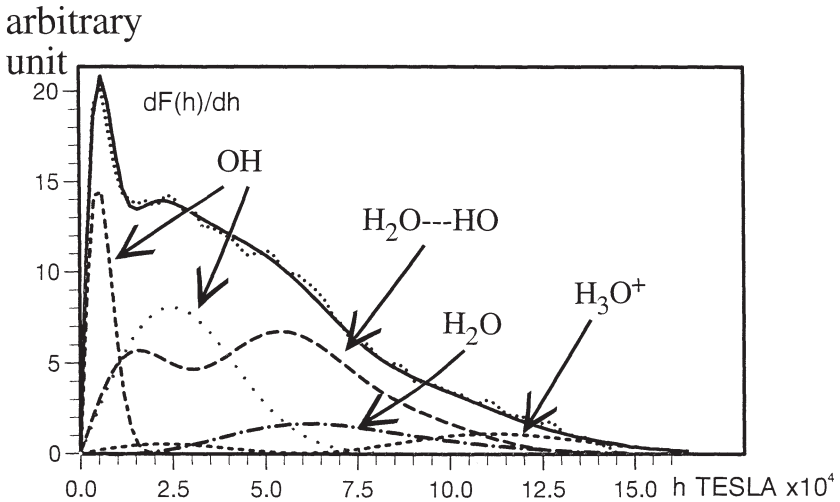

Figure 8. ^{1}H broad-line NMR spectra of ASA LS with $H_{tot.}/Al_{(4)} = 3.04$: (· · ·) experimental, (—) simulated, and partial contributions.

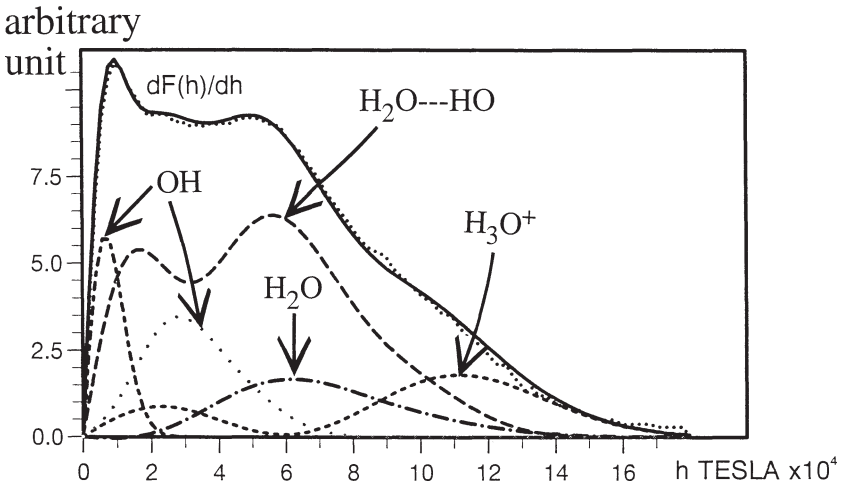

Figure 9. ^{1}H broad-line NMR spectra of ASA LS with $H_{tot.}/Al_{(4)} = 3.70$ equilibrated in air: (···) experimental, (—) simulated, and partial contributions.

Table 3
Oxyprotonated species concentrations (±10%) per Al atom tetra- and penta-coordinated to O atoms, denoted $Al_{(4+5)}$, in ASA HS, from simulations of ^{1}H broad-line NMR spectra.

$H_{tot.}/Al_{(4+5)}$	$H_3O^+/Al_{(4+5)}$	$(H_2O\cdots HO)/Al_{(4+5)}$	$[H_3O^+ + (H_2O\cdots HO)]/Al_{(4+5)}$	$H_2O/Al_{(4+5)}$[a]	$OH/Al_{(4+5)}$[b]	$OH_{anhyd.}/Al_{(4+5)}$	$H_2O_{ads.}/Al_{(4+5)}$
4.30	0.35	0.69	1.04	0.46	0.33 (0.22)	1.37	1.51
4.30	0.41	0.94	1.35	0	0.24 (0.19)	1.59	1.35
2.77	0	0.70	0.70	0	0.67 (0.28)	1.35	0.70
2.48	0	0.47	0.47	0	1.05 (0.28)	1.53	0.47

[a] Not interacting with OH groups.
[b] Not interacting with water; ( ) paired OH.

As already mentioned in the introduction, bas groups of ASA are not stable when dehydrated [5,11]. This makes the study of this kind of sample by ^{1}H broad-line NMR more difficult than that of zeolites. For zeolites, the bas concentration is known from both the framework Si/Al ratio and the simulation of the ^{1}H MAS NMR spectrum of the "anhydrous" sample. For "anhydrous" ASA, there is no ^{1}H MAS signal for bas groups, as seen above. The maximum concentration of the bas groups (re)formed by hydration (figure 1) is limited, a priori, by the smaller of the Si or $Al_{(4)}$ concentrations if the relative locations of Si and $Al_{(4)}$ are favourable. The ^{27}Al MAS NMR spectrum of HS shows a small concentration of $Al_{(5)}$ (or $Al_{(4)}$ with lower symmetry [19]) that we assume, like $Al_{(4)}$, to be able to (re)form some bas. The maximum possible bas concentration is therefore equal to that of: (i) the sum of those of $Al_{(4)}$ and $Al_{(5)}$, denoted $Al_{(4+5)}$, if $Si/Al_{(4+5)} > 1$; (ii) the number of Si if $Si/Al_{(4+5)} < 1$. The formula of the fully hydrated samples, per $Al_{(4+5)}$ or $Al_{(4)}$ for HS or LS, respectively, can be calculated from the chemical formula given in section 2 and from the results of ^{27}Al MAS NMR; they are:

$$7.3\ \text{Si},\quad 1\ Al_{(4+5)},\quad 4.3\ \text{H}\quad \text{for HS};$$

$$1.06\ \text{Si},\quad 1\ Al_{(4)},\quad 3.7\ \text{H}\quad \text{for LS}.$$

The result is that the numerical values must be expressed per $Al_{(4+5)}$ for HS. For LS, the Si and $Al_{(4)}$ concentrations are equal within the limit of the accuracy; the results will be normalized to $Al_{(4)}$. The specific surface areas of both samples are compatible with bas to be accessible to water.

For HS, the concentrations of the species and the typical H–H distance parameters for the spectrum simulations are given in tables 3 and 1, respectively. The concentrations are denoted $H_{tot.}/Al_{(4+5)}$, $H_3O^+/Al_{(4+5)}$, $(H_2O\cdots HO)/Al_{(4+5)}$, $[H_3O^+ + (H_2O\cdots HO)]/Al_{(4+5)}$, $H_2O/Al_{(4+5)}$, $OH/Al_{(4+5)}$, $OH_{anhyd.}/Al_{(4+5)}$, $H_2O_{ads.}/Al_{(4+5)}$, for total H atoms, hydroxonium ions, hydrogen-bonded complexes, sum of the concentrations of hydroxonium ions and hydrogen-bonded complexes, water molecules not interacting with OH groups, OH groups not interacting with water, OH groups of "anhydrous" samples, "adsorbed" H_2O. Therefore, the $OH_{anhyd.}/Al_{(4+5)}$ value includes: (i) remaining isolated and paired OH, (ii) those OH groups which can (re)form bas groups and, subsequently, hydroxonium ions (ionic complexes) and hydrogen-bonded complexes with water; in the same way, $H_2O_{ads.}/Al_{(4+5)}$ includes: (i) the water of these two types of complex, (ii) possibly, water which does not interact with OH. The concentration of water molecules interacting with bas is equal to $[H_3O^+ + (H_2O\cdots HO)]/Al_{(4+5)}$ (table 3). By analogy with the results obtained for other solid acids, it is assumed that only one water molecule interacts with each bas at least as long as the "adsorbed" water concentration is lower than that of $Al_{(4+5)}$. Consequently, the maximum value of $[H_3O^+ + (H_2O\cdots HO)]/Al_{(4+5)}$ should be 1, if the

Table 4
Oxyprotonated species concentrations per Al atom tetra-coordinated to O atoms, denoted $Al_{(4)}$ (±10%) in ASA LS, from the simulations of ^1H broad-line NMR spectra.

$H_{tot.}/Al_{(4)}$	$H_3O^+/Al_{(4)}$	$(H_2O\cdots HO)/Al_{(4)}$	$[H_3O^+ + (H_2O\cdots HO)]/Al_{(4)}$	$H_2O/Al_{(4)}$[a]	$OH/Al_{(4)}$[b]	$OH_{anhyd.}/Al_{(4)}$	$H_2O_{ads.}/Al_{(4)}$
3.70	0.32	0.61	0.93	0.27	0.37 (0.34)	1.30	1.20
3.04	0.16	0.50	0.65	0.23	0.62 (0.58)	1.28	0.89

[a] Not interacting with OH groups.
[b] Not interacting with water; ( ) paired OH.

bas concentration is correctly assumed. The result is that the simulation of HS equilibrated in air ($H_{tot.}/Al_{(4+5)} = 4.30$), for which $[H_3O^+ + (H_2O\cdots HO)]/Al_{(4+5)}$ is found to be 1.35 (table 3, line 2), must be rejected. Only the other simulation obtained for this sample, giving $[H_3O^+ + (H_2O\cdots HO)]/Al_{(4+5)}$ equal to 1.04, is acceptable, and HS contains the maximum possible concentration of bas. The corresponding value of $H_3O^+/Al_{(4+5)}$ is equal to 0.34 (±10%) (table 3), which is the "acidity coefficient", χ_a.

For LS in each of its two hydrated states ($H_{tot.}/Al_{(4)}$ equal to 3.70 and 3.04, table 4), water molecules not interacting with OH groups are present at about the same concentration (0.25). For the fully hydrated sample, $[H_3O^+ + (H_2O\cdots HO)]/Al_{(4)}$ is equal to 0.93. As the corresponding $H_3O^+/Al_{(4)}$ value is 0.32, the same χ_a value of 0.34 (±10%) is obtained for LS and HS.

4. Discussion

As mentioned in section 2, hydrated samples were prepared either by only partial dehydration or by total extraction of the molecular water (in principle, maintaining the concentration of OH groups) followed by water adsorption. It can now be proved that the number of OH groups does not change. Indeed, the results show that for each sample, whatever its hydration level, the simulations of the spectra give the same value (±10%) of OH groups present in the corresponding "anhydrous" sample. They are $OH_{anhyd.}/Al_{(4+5)} = 1.46$ for HS (table 3) and $OH_{anhyd.}/Al_{(4)} = 1.29$ for LS (table 4).

The paired OH groups (tables 1–4) indicate the presence of geminal silanols, $Si(OH)_2$, already shown in these samples by ^{29}Si MAS and CP-MAS NMR [5], in silica [3,21] and in H-ZSM-5 zeolites with high Si/Al ratios [22]. The corresponding intra-pair H–H distance is then 230–240 pm.

Two differences between the two families of ASA are noted, when the samples are less hydrated than in their equilibrated state in air: (i) the (re)formed bas give only the hydrogen-bonded complexes with water at the HS surface (tables 1 and 3), though hydroxonium ions are also formed in the case of LS (tables 2 and 4); (ii) water, not interacting with OH groups, is absent from the HS sample, but present for LS. Moreover, the concentration of these "free" water molecules of LS is constant, $0.25/Al_{(4)}$, for the two $H_2O_{ads.}/Al_{(4)}$ values of this study.

The most hydrated HS and LS samples both contain some water molecules not interacting with the remaining OH groups. These OH groups do not belong to bas and would not be able to give them. The maximum concentration of bas groups, equal to that of $Al_{(4+5)}$ or $Al_{(4)}$ for HS or LS, respectively, is reached for both ASA samples when they are fully hydrated in air.

The χ_a value, the hydroxonium concentration per bas when one water molecule interacts with each bas, can be found from the results (tables 3 and 4) for the highest possible concentration of bas groups, i.e., for the stable hydrated samples in air. The same value is obtained for HS and LS, $0.34 \pm 10\%$. This value is a little larger than that obtained for H-mordenites [12,17] and equal to those of some H-faujasites [12,23], the framework Si/Al ratios of these zeolites, about 10, being large enough for maximum acid strength [24].

5. Conclusion

The study of amorphous silica–alumina samples in the presence of adsorbed water, using ^1H NMR, both MAS at room temperature and broad-line at 4 K, represents a limiting attempt to use these methods. One reason for this limitation is the poor resolution of the broad-line spectra, compared to most of those of crystallized samples. However, the main reason is related to the fact that acidic bridging OH groups, stable when hydrated, are reversibly destroyed by dehydration. Quantification of the bas is, therefore, impossible using ^1H MAS NMR and, consequently, the broad-line spectra cannot be interpreted on the basis of an accurate prenormalization of the H atoms of the samples.

However, ^1H broad-line NMR provides interesting and consistent results on amorphous silica–aluminas. For two ASA samples with very different Si/Al ratios (one larger and the other smaller than 1), the acidity coefficient, χ_a, equal to the hydroxonium concentration per bas when one water molecule interacts with each bas, can be estimated to be ca. $0.34 \pm 10\%$. This value was measured for the higher hydration level, when the bas concentration is maximum. The acid strength of amorphous silica–aluminas is, therefore, comparable to that of H-zeolites, mordenites and faujasites, with Si/Al ratios large enough for maximum acid strength.

In spite of the difficulty of this particular case due to the nature of the samples, the association of both ^1H NMR techniques, broad-line at 4 K and MAS at room temperature, proves again to be a powerful tool for the study of the acidity of solids.

Appendix

A.1. Sample preparation

Samples were usually vacuum "shallow-bed" pretreated (10^{-2} Pa) at temperature low enough to make them "anhydrous", i.e., in principle dehydrated, but containing the initial OH groups. For slow dehydration, the temperature was raised gently to the maximum, and maintained overnight at this temperature, 673 and 623 K, for zeolites and amorphous silica–aluminas, respectively. After cooling, water vapour was adsorbed stepwise at 300 K, the initial pressure being each time less than a third of the saturation pressure. The amount of water was determined by volumetric and gravimetric measurements. Since the water adsorbed in this way was not generally distributed homogeneously, the samples were homogenized at 383 K for 15 h. The samples were then transferred to 5 mm thin-walled tubes already connected to the reactor. These tubes were sealed away from the reactor. In order to get their axial symmetry good enough for MAS experiments, they were sealed again using a microflame while spinning at a few Hz. The same ampules were used for both ^{1}H NMR techniques.

A.2. ^{1}H NMR spectrum recording

Room temperature MAS [25] was performed with a 400 MHz Bruker spectrometer and 3 or 4.5 kHz spinning of the samples; the repetition time was 20 s for "anhydrous" samples and 5 s if water had been adsorbed.

For broad-line NMR at 4 K (under "rigid-lattice" conditions), the basis of the apparatus was a cw DP60 Varian (1.4092 T) used with a home-made probe. The quality coefficient of the single coil was about 60. The probe can be immersed in liquid helium. Its particularity is that it can be adapted and tuned at the working temperature, using sliding cylindrical capacitors controlled from the outside. Under these conditions, the coaxial wire (50 Ω) is no longer part of the active circuit. The amplitude of the radiofrequency magnetic field is small (a few 10^{-7} T) to avoid resonance saturation. The probe is connected to a 90° power divider/combiner. Phase-sensitive detection is used. The sweep of the B_0 field is 5×10^{-3} T on the resonance area. In order to obtain derivative spectra relative to B_0, this field is modulated at 20 Hz, with a peak-to-peak amplitude of 6.8×10^{-5} T. The spectra are accumulated (60–300 times, depending on the spectrum quality), each scan lasting 100 s with 5 s between scans. We have assumed, from previous experiments, that the distribution of species concentrations does not change between 300 and 4 K. *Half-derivative spectra are shown in the figures.*

The basic physical effect is a dipolar magnetic interaction between any couple of two protons, proportional to r^{-3}, where r is the distance between the protons [14]. This effect enables us to measure quantitatively the concentrations of the species formed by interaction of molecular water with bas groups (equation (1)):

$$\begin{aligned} \mathrm{SiO(H)Al} + \mathrm{H_2O} &\rightleftharpoons \mathrm{H_2O\cdots HO(Si)(Al)} \\ &\rightleftharpoons \mathrm{H_3O^+} + \mathrm{(SiOAl)^-} \end{aligned} \tag{1}$$

The broad-line spectra were simulated by means of a program, written in Fortran. They correspond to weighted sums of the contributions of the various species, for which the following magnetic configurations were calculated: (i) H_2O, a $\boldsymbol{r}$-distant two-spin configuration [25]; (ii) $H_2O\cdots HO$ and H_3O^+, considered as deformed: a magnetic configuration with three spins at the vertices of an isosceles triangle [26,27], where $\boldsymbol{r}$ is the base and $\boldsymbol{r}'$ the equal sides (see below); (iii) H_3O^+ assumed to have C_{3v} symmetry, a magnetic configuration with three $\boldsymbol{r}$-distant spins at the vertices of an equilateral triangle [28,29]; (iv) OH, either a two-spin configuration [30] (if some OH groups are paired) or an absorption with a pure Gaussian or Lorentzian shape located at the centrum of the absorption spectrum, because the corresponding r distances are large relative to $\boldsymbol{r}$ and $\boldsymbol{r}'$; a Gaussian function corresponds to protons "statistically" distributed and a Lorentzian function to "diluted" spins [31]. A linear combination of these two functions can be used. Each of the corresponding functions (except for the Gaussian and the Lorentzian) is convoluted by a Gaussian, which allows for the interactions between the hydrogen nuclei of the configuration and (i) those belonging to neighbouring configurations, (ii) the other nuclei with non-zero spin in the vicinity (mainly ^{27}Al in the present case). When the nuclear interaction between Al and H is small relative to the interconfiguration interaction between protons, the parameter of each Gaussian is related to a distance $\boldsymbol{X}$, which is close to the shortest distance between a proton of the configuration considered and a proton outside it.

When a magnetic configuration with three protons at the vertices of an isosceles triangle is used, the $\boldsymbol{r}$ value is always found typical of a water molecule (between 145 and 165 pm, usually between 155 and 165 pm). When $\boldsymbol{r}'/\boldsymbol{r}$ is $\leqslant$1.1, deformed hydroxonium ions are detected. No $1.1 < \boldsymbol{r}'/\boldsymbol{r} < 1.4$ values have been observed. For larger $\boldsymbol{r}'/\boldsymbol{r}$, the internal O–O distance of $H_2O\cdots HO$ is calculated assuming C_{2v} symmetry for the groups and OH distances of 100 pm; the presence of hydrogen-bonded complexes is claimed from usual O–O distances. Larger O–O distances than those corresponding to the presence of hydrogen bonds are sometimes obtained. In such cases, the total concentrations of OH and H_2O, either using a three-H configuration and, possibly, that of H_2O or OH, or only distinct configurations for these last species, are identical. The $\boldsymbol{r}'/\boldsymbol{r}$ values corresponding to the simulations always lead to clear conclusions.

The shape of the half-derivative spectra of H_2O gives a maximum about 6×10^{-4} T; those of H_3O^+ two, especially a characteristic one at about $10\text{–}12 \times 10^{-4}$ T, the other being near the origin, where are also those of OH groups. The

spectra of $H_2O\cdots HO$ usually show two maxima, near the origin and from 4 to 6 T, but the relative intensities of these signals do not correspond to that of the same concentration of magnetically independent H_2O and OH [27].

The results are expressed with a calculation basis, either a unit cell for zeolites or, more usually, a Brønsted acid site. The total number of protons is equal to the number of all kinds of OH groups of the "anhydrous" samples plus twice the number of adsorbed water molecules. Acceptable values of $\boldsymbol{X}$ must be greater than (or at least equal to) those of $\boldsymbol{r}$ and $\boldsymbol{r}'$ when the influence of interactions of ^{27}Al nuclei is negligible. Moreover, since the number of independent parameters for each simulation is high, it was generally assumed that no new water molecule was formed from OH groups nor OH groups obtained by the dissociation of adsorbed water molecules. In the usual range of $\pm 10\%$ accuracy on the species concentrations and the above constraints, the simulation is unique due to the individual shape of the spectrum of each magnetic configuration and the abscissa value of each of their maxima or minima. Due to difficulties in determining a convenient base and for the first time, for the "high silica" (HS) amorphous silica–alumina, equilibrated in air, two distinct simulations of the experimental spectrum were acceptable. This point is discussed in detail.

References

[1] B.C. Gates, J.R. Katzer and G.C.A. Schuit, *Chemistry of Catalytic Processes*, McGraw-Hill Chem. Eng. Series (McGraw-Hill, New York, 1979).
[2] A. Corma, Chem. Rev. 95 (1995) 559.
[3] G.E. Maciel and P.D. Ellis, in: *NMR Techniques in Catalysis*, eds. A.T. Bell and A. Pines (Dekker, New York, 1994) p. 231 and references therein.
[4] Eckert, in: *NMR Techniques in Catalysis*, eds. A.T. Bell and A. Pines (Dekker, New York, 1994) p. 218 and references therein.
[5] C. Dorémieux-Morin, C. Martin, J.M. Brégeault and J. Fraissard, Appl. Catal. 77 (1991) 149.
[6] M. Hunger, D. Freude, H. Pfeifer, H. Bremer, M. Jank and K.P. Wendlandt, Chem. Phys. Lett. 100 (1983) 29.
[7] M. Hunger, D. Freude and H. Pfeifer, J. Chem. Soc. Faraday Trans. 87 (1991) 657.
[8] I. Wolf and D. Freude, Micropor. Mater. 5 (1995) 69.
[9] D. Freude, H. Ernst and I. Wolf, Solid State Nucl. Magn. Reson. 3 (1994) 271.
[10] D. Freude, Chem. Phys. Lett. 235 (1995) 69.
[11] C. Dorémieux-Morin, P. Batamack, C. Martin, J.M. Brégeault and J. Fraissard, Catal. Lett. 9 (1991) 403.
[12] C. Dorémieux-Morin and J. Fraissard, J. Japan Petrol. Inst. (Sekiyu Gakkaishi) 40 (1997) 355 and references therein.
[13] P. Batamack, C. Dorémieux-Morin, J. Fraissard and D. Freude, J. Phys. Chem. 95 (1991) 3790 and references therein.
[14] G.E. Pake, J. Chem. Phys. 16 (1948) 327.
[15] P. Batamack, C. Dorémieux-Morin, R. Vincent and J. Fraissard, J. Phys. Chem. 97 (1993) 9779 and references therein.
[16] L. Heeribout, V. Semmer, P. Batamack, C. Dorémieux-Morin, R. Vincent and J. Fraissard, Stud. Surf. Sci. Catal. 101 (1996) 831.
[17] L. Heeribout, V. Semmer, P. Batamack, C. Dorémieux-Morin and J. Fraissard, J. Chem. Soc. Faraday Trans. 91 (1995) 3933.
[18] J.P. Gilson, G.C. Edwards, A.W. Peters, K. Rajagopalan, R.F. Wormsbecher, T.G. Roberie and M.P. Shatlock, J. Chem. Soc. Chem. Commun. (1987) 91.
[19] J.J. Fitzerald, A. Hamza, C.E. Bronnimann and S.F. Dec, Solid State Ion. 32/33 (1989) 378.
[20] P. Batamack, C. Dorémieux-Morin, R. Vincent and J. Fraissard, Micropor. Mater. 2 (1994) 515.
[21] C. Dorémieux-Morin, L. Heeribout, C. Dumousseaux, J. Fraissard, H. Hommel and A.P. Legrand, J. Am. Chem. Soc. 118 (1996) 13040.
[22] L. Heeribout, C. Dorémieux-Morin, J.-P. Nogier, R. Vincent and J. Fraissard, Micropor. Mesopor. Mater., in press.
[23] Unpublished results.
[24] D. Barthomeuf, Math. Chem. Phys. 17 (1987) 49.
[25] D. Freude, Stud. Surf. Sci. Catal. 52 (1989) 169 and references therein.
[26] E.R. Andrew and N.D. Finch, Proc. Phys. Soc. 70B (1957) 980.
[27] C. Dorémieux-Morin, J. Magn. Res. 21 (1976) 419; 33 (1997) 505.
[28] E.R. Andrew and R.J. Bersohn, J. Chem. Phys. 18 (1950) 159.
[29] R.E. Richards and J.A.S. Smith, Trans. Faraday Soc. 48 (1952) 675.
[30] A.L. Porte, H.S. Gutowsky and J.E. Boggs, J. Chem. Phys. 36 (1962) 1695.
[31] A. Abragam, *Les Principes du Magnétisme Nucléaire* (Presses Universitaires de France, Paris, 1961).